Infrared Spectra of Poly(ethylene Terephthalate) Yarns. Fitting of Spectra, Evaluation of Parameters, and Applications

H. M. HEUVEL and R. HUISMAN, *Enka Research Institute Arnhem, Fibre Research Department, 6800 AB Arnhem, The Netherlands*

Synopsis

A quantitative model for fitting infrared spectra of polyethyleneterephthalate samples over the region from 1100 to 720 cm^{-1} has been evaluated. The absorbance was described as the sum of a linear base line and a set of symmetrical bell-shaped Pearson VII curves. Using this model, experimental transmission spectra of yarns, measured with the electric vector parallel and perpendicular to the fiber axis, were fitted. It was found that each of the trans bands near 972 and 845 cm^{-1} consists of two components, a narrow and a broad one. These two components represent the crystalline and amorphous phases respectively. The band due to the out of plane benzene ring C—H deformation vibration at about 875 cm^{-1} appeared also to be composed of two contributions. In this case, the narrow component was found to be due to molecules having interactions with direct neighbors. So this narrow component not only contains the molecules in the crystalline phase but also those forming part of bundles which are too small to be detected by x-ray diffraction. For a detailed insight into the molecular arrangement of the amorphous regions, the infrared detection of *trans*-guache transitions, fold content, detection of bundlelike structures, and molecular stress on tie molecules turned out to be of great practical importance. The structural details, which can be revealed by the infrared technique, cannot be obtained by other means. The potential of the method is illustrated with some practical examples.

INTRODUCTION

The physical structure of semi-crystalline polymers can be described adequately by a two-phase model, consisting of alternating amorphous and crystalline regions. Using a combination of measuring techniques such as density, X-ray diffraction, pulse propagation, birefringence, and thermal analysis, a rather good picture of the parameters involved in such a model can be obtained.[1] These parameters proved quite useful in understanding the influence of process conditins on yarn properties.[2,3] A problem, however, remains a more detailed picture of the amorphous regions. Whereas the structure of the crystals can be studied in detail, using X-ray diffraction techniques, the information about the amorphous regions is limited to rough overall quantities such as average orientation of the molecules or average size of the amorphous regions.

In Figure 1 the usual model for an amorphous region as encapsulated between two crystals is depicted. As a first approximation, the crystals can be considered to be stiff blocks. Therefore, it is clear that the molecular arrangement in the amorphous regions is of ultimate significance for the mechanical behavior of a yarn. In this respect two features are supposed to be of major importance. The first is the folding of the molecules at the

Journal of Applied Polymer Science, Vol. 30, 3069–3093 (1985)
 CCC 0021-8995/85/073069-25$04.00

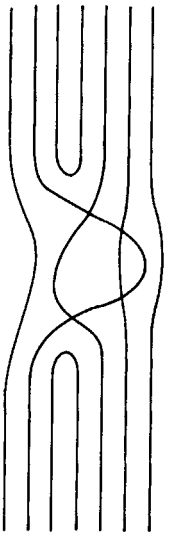

Fig. 1. Two phase model for a PET fiber.

boundaries of the crystals. As folded chains cannot contribute to modulus or strength, they should be avoided as much as possible. The second is the tie-chain length distribution. The molecules running from one crystal to the other, may consist of many or of only a few monomer units. If the distribution is broad, the molecules will not cooperate in bearing a load exerted on the yarn. Successive breakage or slippage of one molecule after the other will take place, resulting in low strength and modulus. So the influence of process parameters on this tie-chain length distribution has to be studied. From the literature evidence has emerged that infrared spectroscopy is able to provide information on these two structural features.

In 1970 Statton, Koenig, and Hannon[4] associated the folding of PET molecules with the 988 cm^{-1} band in infrared spectra. So the first aspect can be studied in this way. The other one, relating to tie-chain length distribution, is much more complicated and requires a detailed analysis of infrared spectra of yarns elongated to various extents. During elongation the shape of the molecules in the amporphous regions will change in a different way depending on their tie-chain length.

This is schematically illustrated in Figure 2, where the originally taut molecule a can only adapt to the elongated situation by an increase of valence angles or breakage. Molecule b can bridge the increased gap by straightening the original bends by rotational transitions from gauche to trans. The length of molecule c is such that it can keep a considerable part of the original curvatures also in the elongated state. So this molecule still contains, in the elongated state of the yarn, a considerable amount of the gauche conformer. As infrared spectroscopy can detect changes of the valence angles,[5-10] as well as transitions from gauche to trans,[11-16] a more detailed picture of the tie-chain length distribution can thus be obtained.

The aim of this work was to develop an infrared technique to study the aforementioned aspects on a quantitative basis. The requirement to study yarns at various strain levels necessitated the development of a special

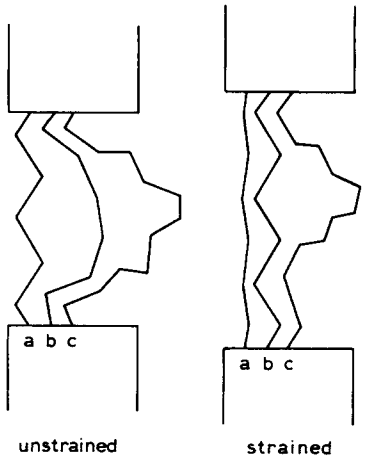

Fig. 2. Response of different tie-molecules to straining.

winding technique. The yarns had to be wound in such a way that on both sides of a small metal frame a perfectly smooth layer with a thickness of one monofilament was formed. As such layers scatter the infrared radiation to a very large extent, a spectrometer with excellent sensitivity in the region of low transmittance was required. No embedding liquid or KBr plate was used for theoretical as well as practical reasons. Finally a computer program had to be developed to describe quantitatively the transmittance spectra obtained in order to get parameter values which can be related to process conditions and yarn properties. To this end, the infrared spectra of a series of yarns, covering a wide range of different physical structures, were used. Thus a model could be developed which may be considered to be generally applicable to infrared spectra of PET samples.

The main part of the underlying paper presents the fitting of spectra and the interpretation of results in physical terms. Subjects specifically related to problems due to the special shape of yarn samples[15] are dealt with in separate appendices in order to avoid distraction from the infrared subject proper.

EXPERIMENTAL

Types of Yarn

For the development of the model use was made of two different series of yarns which had to cover quite a range of physical structures. So a variety of crystallinities, amorphous and crystalline orientations, tie-chain length distributions, etc., had to be represented. As we were also interested in the molecular response on straining, yarns elongated to various extents were included as well. Hence the following series have been chosen:

A. A set of undrawn yarns, wound at a large range of winding speeds, offers a number of extremely different structures varying from totally amorphous to partially crystalline with very well developed crystals. The set consists of yarns, dtex 167f30, wound at speeds varying from 2500 to 6000 m/min. The specific viscosity, being 0.63, was measured as a solution of 1

g PET in 100 g *m*-cresol at 25°C. The structure of the yarns has been extensively described elsewhere.[3] The most relevant parameters are summarized in Table I.

B. Set B contains samples of tyre yarn wound at elongations varying from 0 to 6%. The latter percentage is the highest attainable for this yarn with respect to breakage of filaments during winding on the infrared frames. This is about half the elongation at break occurring in a normal stress–strain testing machine. The count of the yarn is dtex 1100f192 and the specific viscosity in *m*-cresol 0.89 at 25°C.

To present some more applications, a third set of yarns will be discussed which has not been used for the development of the infrared model. As the literature[16,17] reveals an increasing interest in structural differences between yarns, drawn from as-spun yarns wound at different speeds, some examples in this field will also be presented. These yarns will be referred to in the following as set C.

C. The yarns have been drawn from as-spun yarns wound at 500, 2000, and 4000 m/min. Two-stage drawing was performed at a pin temperature of 86°C and afterdrawing took place in a steambox of 245°C. The draw ratio was adjusted to such a value that the three yarns had the same elongation at break of 9.5%. Each of these three drawn yarns was wound at a variety of elongations. The total count was dtex 1150f200 and the specific viscosity about 0.88 at 25°C for solutions containing 1 g polymer in 100 g *m*-cresol.

Winding

For these quantitative infrared measurements the yarns had to be wound in such a way that on both sides of a small metal frame a smooth layer of parallel monofilaments was formed with a minimum of air gaps and overlaps. Thirty filaments out of the yarn bundle are arranged parallel, forming

TABLE I[a]

Winding speed (m/min)	Volume fraction crystallinity	Crystalline orientation factor f_c	Amorphous[a] orientation factor f_a
2500	0		0.155
3000	0		0.246
3500	0		0.367
4000			
4250			
4500			
4750	0.106	0.965	0.602
5000	0.155	0.972	0.626
5500	0.209	0.976	0.650
6000	0.242	0.979	0.693

[a] These orientation factors are based on pulse propagation measurements and differ from those obtained from birefringence measurements.[17] This is due to the fact that the pulse propagates along the taut tie molecules, resulting in higher orientation factors than those based on the average tie-chain length as obtained by optical birefringence. Both types of measurements have their own merits, and in principle the combination can provide information on the tie-chain length distribution.

a proper ribbon which can be elongated to the required extent. After stress–relaxation the yarn is wound at constant stress by rotating the frame. At each half turn of the frame, the ribbon of filaments is displaced laterally in such a way that a smooth, closed layer without overlap forms. For a bundle of dtex 170f30 this traversing on a frame with a width of 18 mm causes an angle of 2° between the filament directions on both sides of the frame. This value is low enough to avoid disturbance of the dichroic measurements. After winding, the samples have to be examined under the microscope for fiber overlaps and air gaps.

Our experience with this technique is limited to straight yarns with circular cross sections. Probably also multilobal yarns can be handled in this way. In the infrared measurement reflection and divergence will be different then, which affects only the base line and not the peaks. In winding textured yarns all crimps must be straightened.

Recording the Spectra

The spectra of the PET yarns are recorded with a Perkin-Elmer 580 ratio recording apparatus. This instrument is very sensitive, especially in the regions of low transmittance, which is required for obtaining yarn spectra with sufficient accuracy. The low transmittance is due to the fact that the round cross section of the yarns causes extreme scattering of the infrared radiation, as discussed extensively in Appendix A. Scanning conditions were optimized to the best signal-to-noise ratio and consequently a moderate resolution (3.6 cm^{-1}) as well as a slow scanning speed (10 cm^{-1}/min) had to be accepted. For our spectra this moderate resolution had no harmful effect and the slow scanning speed could be compensated for by using the automatic sample changer which provided the possibility of measuring series of samples overnight. The yarns were scanned with both parallel and perpendicularly polarized infrared radiation. Both types of spectra were recorded because not only information about isotropic quantities was required but also about orientation phenomena.

Besides the yarn spectra proper, also zero-transmittance lines were needed for taking into account very precisely the actual 0% transmittance values. These zero-transmittance lines were obtained by putting a metal plate in the infrared beam. During the measurement of a series of samples, recording of the yarn spectra and of the zero-transmittance lines succeeded each other alternately. All information was recorded both graphically and in digitized form. For the digitized recording use was made of a magnetic tape device which, for each integer wavenumber, automatically recorded the actual transmittance value. The digitized form of each spectrum contained about 400 data points. Also the wavenumber, corresponding to the first transmission value, was recorded on the magnetic tape because it was needed for the construction of the wavenumber axis by the computer.

As the reproducibility of the wavenumbers is very essential for the application of the fitting model to be proposed, this construction of the wavenumber axis has to be very reliable. In case of moderate wavenumber reproducibility, the construction can be based on the position of the 7g2.3 cm^{-1} benzene band which is found to have a constant peak position. First

only a part of the spectrum around this bond is fitted. To the peak position found the wavenumber 7g2.3 cm^{-1} is assigned. Based on this value and on the known interval between successive measuring points the wavenumber axis can be constructed.

Computations

Use was made of a CDC 6600, an IBM 3033 (double precision) and in the vast majority of cases of a Harris H500 computer.

DEVELOPMENT OF A FITTING MODEL

Initial Fitting

In Figure 3 examples of a parallel and a perpendicular spectrum are presented. To fit the spectra, the transmission was described as

$$T = 10^{-A} = 10^{-[p+q\sigma+\sum_{i=1}^{n} P_i(\sigma)]} \tag{1}$$

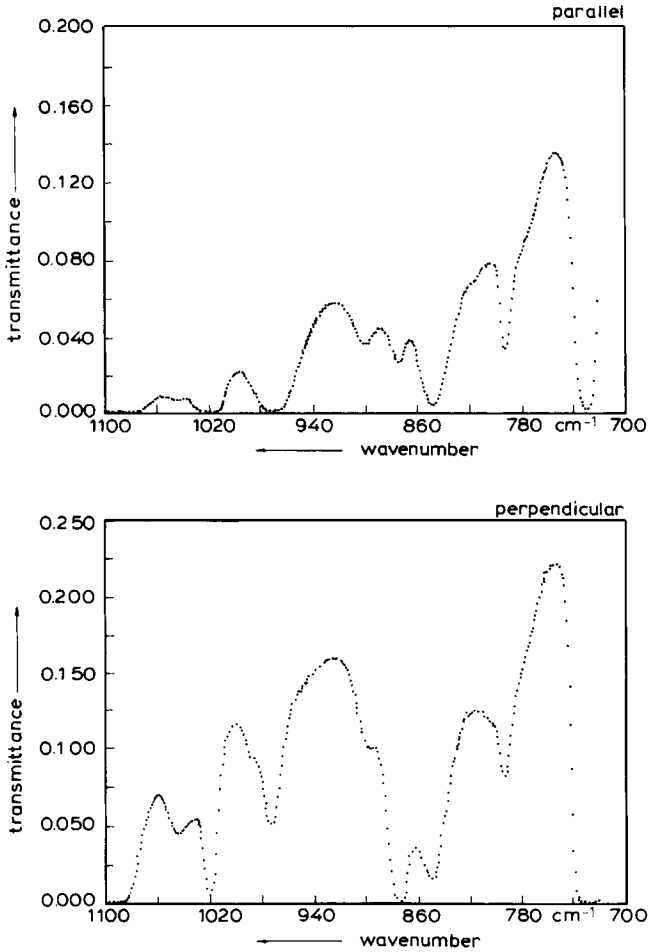

Fig. 3. Digitized parallel and perpendicular spectrum of a PET yarn.

where T is the transmission, A the absorbance, $p + p\sigma$ the equation assumed for the base line, $P(\sigma)$ the symmetrical bell-shaped Pearson VII function,[18,19] and n the number of these curves needed for fitting the spectra.

The Pearson VII function contains four parameters. Its advantage over many other functions, such as the Gausz and Cauchy functions, is that halfwidth and tail can be varied almost independently. Also for the quantitative description of X-ray diffractometer traces this function was applied successfully.[18,19] Further details about formula (1) are presented in Appendix B.

In a first trial to fit the experimental traces with the mathematical expression presented, use was made of a number of Pearson VII lines equal to the number of peaks showing up in the experimental traces. Fits were calculated for all 17 yarns of sets A and B. Regions of misfitting were compared and for those where practically all yarns had too low absorbances, i.e., too high transmittance values, extra Pearson VII lines were introduced. So, using one consistent model for all yarns, fits could be reached which were quite satisfactory from a numerical point of view.

Reduction of the Number of Parameters

For a satisfactory description of the infrared spectra over the region 1100-700 cm^{-1}, more than 20 Pearson VII lines were needed for both the parallel and perpendicular spectra. Consequently, a very large number of parameters was involved. Not only were the computations very time-consuming, but also the accuracy of most of the calculated parameters was poor. Therefore, the possibility of fixing peak positions, halfwidths and shape factors had to be considered. All parameters which did not vary significantly throughout both series of yarns involved were fixed at constant values. It turned out that fixation could be be applied to so many parameters that the problems mentioned before could be considerably reduced. As the fixed parameter values for parallel and perpendicular spectra were mostly the same, further progress could be reached by fitting both spectra simultaneously. However, not all peak positions, halfwidths, and shape factors could be fixed. The most striking exceptions were the gradual shift of the 972 cm^{-1} peak position as a function of elongation and the dependence of the halfwidth on crystallinity for three lines. These cases will be discussed in the next subsections.

Halfwidth Depending on Crystallinity

In fitting the yarns of series A, it was found that for three of the contributing components the halfwidth decreased significantly with increasing crystallinity. In Figure 4 this decrease in halfwidth is illustrated for the band near 972 cm^{-1}. Analogous effects were observed for the bands at about 875 and 845 cm^{-1}.

As early as 1972 Melveger found that the halfwidth of the 1730 cm^{-1} Raman band decreased with crystallinity[20], as determined from the combination of density and X-ray diffraction measurements.[3] Westra and Wuestman[21] found that the halfwidth of the overtone infrared band at 3430 cm^{-1} decreased proportionally with increasing density. We supposed that

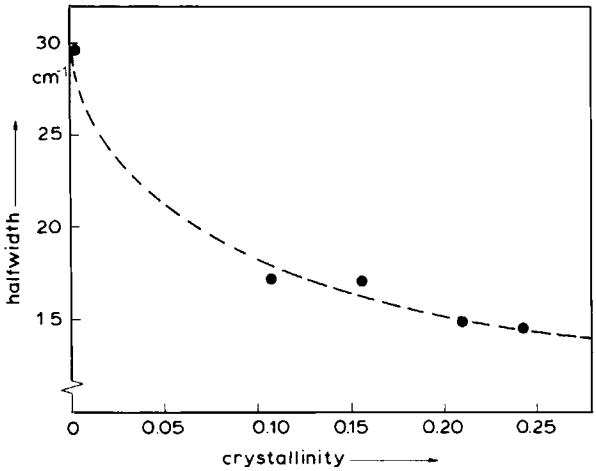

Fig. 4. Decrease of the halfwidth of the 972 cm^{-1} parallel band with increasing crystallinity.

the three bands mentioned before were composed of two components each, one originating from well-ordered, maybe crystalline, regions and the other from less ordered material.

So new fits were calculated with the original three bands, the varying halfwidths being replaced by six, each with constant halfwidth. It turned out that in this way very good fits were obtained with statistically well-determined parameters. Now for all bands of the model constant halfwidth values were used. The originally varying halfwidth of the three bands discussed could be accounted for by varying the ratio between narrow and broad components. As for well-ordered systems, less variation in transition energy is involved, the better ordered regions should be related to the narrow components. The quantitative results for the bands involved are given in Table II. The crystallinity effects have also been found by Koenig,[22] but in a more qualitative way. The concept of "well-ordered" regions has to be investigated for each of the three bands in more detail.

Nature of Ordered Regions Related to the Narrow Components of the 972, 875, and 845 cm^{-1} Bands

In Figure 5 the behavior of the three narrow components is illustrated. On the vertical axis normalized isotropic areas are indicated. This quantity is proportional to the number of molecular species active in that particular

TABLE II

	Peak position (cm^{-1})	Halfwidth (cm^{-1})	Shape factor	Band assignment
About	970	30.0	1.2	Trans
About	972	11.7	1.7	
	877.0	21.0	1.9	Benzene, out of plane
	873.5	9.5	1.2	
	840.5	33.0	1.6	Trans
About	848.5	13.0	1.7	

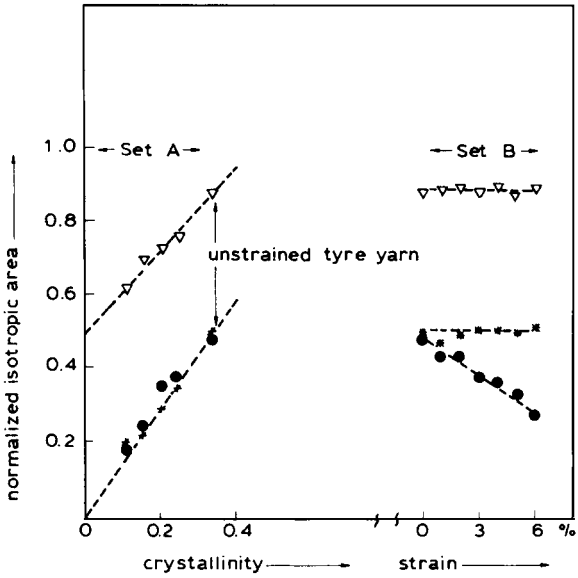

Fig. 5. Dependence of the three narrow components on crystallinity and strain. Bands at: (●) 972 cm^{-1}; (▽) 873.5 cm^{-1}; (*) 848.5 cm^{-1}.

transition, per unit of material involved in the infrared absorption. Details on this point will be discussed in the subsection "normalized isotropic areas". From Figure 5 the following conclusions can be drawn:

972 Band

As long as the molecules are not in a pronounced strained situation, this band is fairly proportional to crystallinity. However, strain has a very pronounced influence on the isotropic area. Although strain on the molecules can cause a shift on this peak position, it is not probable that this would interfere with the isotropic area as it looks reasonable to suppose that all molecules in the crystals are strained in the same way. Consequently, the halfwidth is not likely to be influenced by strain. Possibly the transition probability is not constant. Whatever the reason may be, the sensitivity to strain makes this band less suitable for the determination of crystallinity.

848 Band

This band behaves ideally with respect to crystallinity. The linear relationship is good, and the quantity does not show any appreciable change with strain.

873.5 Band

This band also shows a satisfactory relation with crystallinity, which is in accordance with the literature[23,24] where the band was associated with ordered regions. However, there is a problem with the situation where crystallinity vanishes. Then there still is a considerable amount of molecules

contributing to the narrow "ordered" band. This band can, according to the literature[25] be assigned to the out of plane C—H benzene ring vibration mode. From dichroism it follows that the vibration is nearly perpendicular to the molecular axis. It is supposed now that this vibration, perpendicular to the benzene ring, is extremely sensitive to the presence of other benzene rings in the proximity. This means that in this narrow band all molecules forming part of clusters are active also when these clusters are too small to be detected by X-ray diffraction. There is some experimental support for this hypothesis. In series A, an influence of orientation on thermal crystallization is observed in the region of winding speeds where no crystallization takes place at all.[3] In accordance with the literature[26] it was found that crystallization during heating shifts to lower temperatures at higher winding speeds, as illustrated in Figure 6. This can be ascribed to an improved nucleation caused by an increased orientation. For these yarns also an increase of the narrow 873.5 cm^{-1} band with orientation has been found, supporting the idea that already nuclei show up as ordered regions in this ordered benzene band. The conclusion with respect to this band is therefore that it measures all molecules which are associated with neighbouring molecules. So the broad component has to be assigned to individual, isolated parts of molecules.

Shift of the "972"-Peak Position as Caused by Strain

One of the reasons to start this infrared work was the fact that several investigators, such as Statton and Zhurkov had found that the "972"-band shifted when stress was exerted on the molecules. This important finding was confirmed by our experiments as illustrated in Figure 7. As discussed above, in our case two peaks are involved, one related to the crystalline, the other to the amorphous material. Series B shows a marked decrease of both peak positions with elongation. The fact that the shift of the amorphous part is greater than that of the crystalline parts is in accordance with the lower modulus of the amorphous material, causing a greater elongation. That also a shift was found for the molecules in the relatively stiff crystalline blocks is supported by X-ray diffraction results. These are shown in

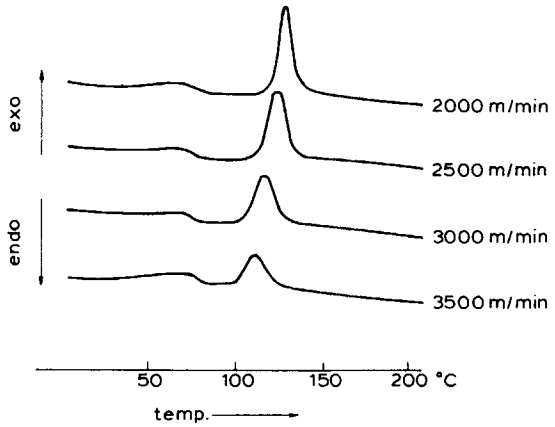

Fig. 6. DSC traces of undrawn yarns wound at various speeds.

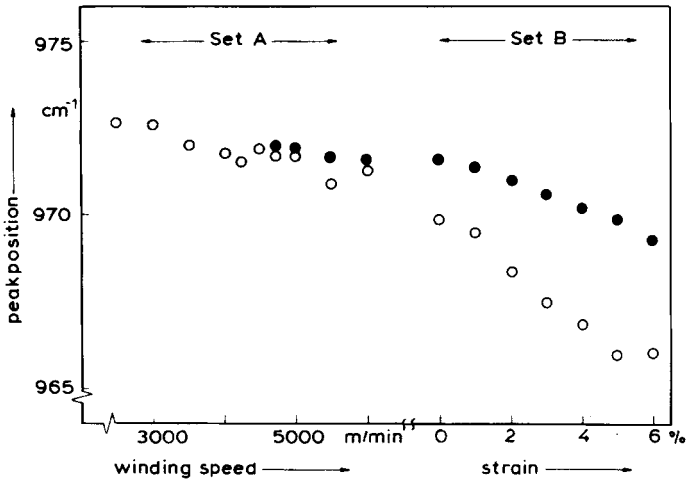

Fig. 7. Influence of stress on the peak positions of the two "972"-components: (●) crystalline; (○) amorphous.

Figure 8, where the height of the crystalline unit cell is given as a function of elongation. From the results of series A, it is clear that also during spinning the amorphous molecules are slightly under stress. This phenomenon is more pronounced at higher winding speeds.

Normalized Isotropic Areas

Isotropic areas are important as they are proportional to the number of molecules active in the vibration transition involved. They are calculated from the parallel and perpendicular spectra as

$$A_{iso} = (A_{\parallel} + 2A_{\perp})/3 \tag{2}$$

where $A_{\parallel}$ and $A_{\perp}$ indicate the integrated areas of the absorbance peaks in the parallel and perpendicular spectras, respectively. Of course these iso-

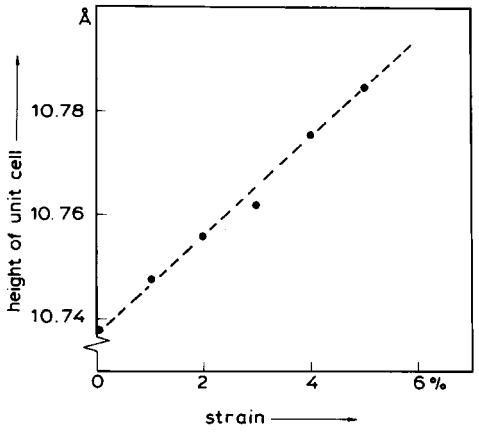

Fig. 8. Effect of strain on the height of the crystalline PET unit cell.

tropic areas increase with the amount of material taking part in the infrared absorption. Hence, in the case of yarns the isotropic areas will increase with the yarn count. Therefore, it has to be expected that for a species which is always present at a constant level in all PET fibers, the isotropic area can be written as

$$A_{iso} = c \cdot t^n \tag{3}$$

where c is a proportionality constant, t the filament count (measure of the number of molecules distributed over the cross section), and n an exponent. As trans, gauche, and folded configurations are not present at constant levels but depend on the physical structure, the most suitable species is the benzene part of the molecule. However, it was shown that the benzene band at approximately 875 cm^{-1} consists of two components which possibly have different transition probabilities. So, for this case, formula (3) has to be written as

$$A_{b,a} + \alpha A_{b,i} = ct^n \tag{4}$$

where $A_{b,a}$ = isotropic area of the narrow benzene band (associated molecules) and $A_{b,i}$ = isotropic area of the broad benzene band (isolated molecules).

The yarns of series A and B have the same filament count but quite different structures. Hence for these yarns a linear relationship between $A_{b,a}$ and $A_{b,i}$ has to be expected. Figure 9 shows that the experimental results are in reasonable agreement with this expectation and the coefficient α is calculated as 0.44. So eq. (4) now becomes

$$A_{b,a} + 0.44A_{b,i} = ct^n \tag{5}$$

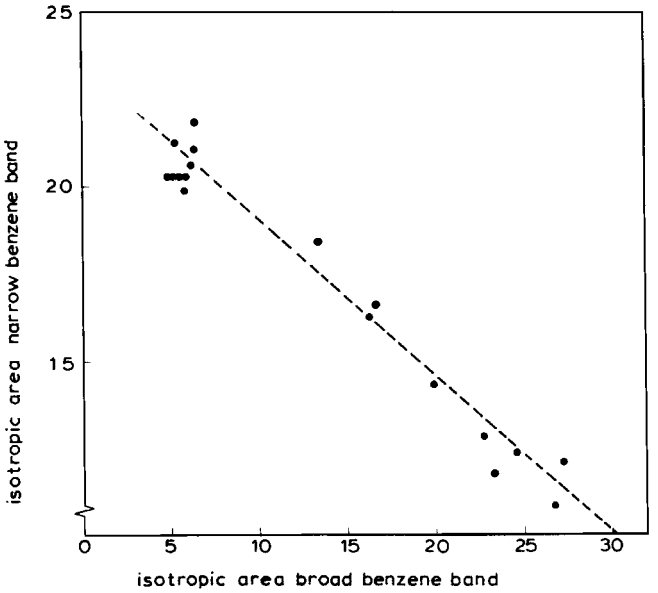

Fig. 9. Relation between the two benzene band components at about 875 cm^{-1}.

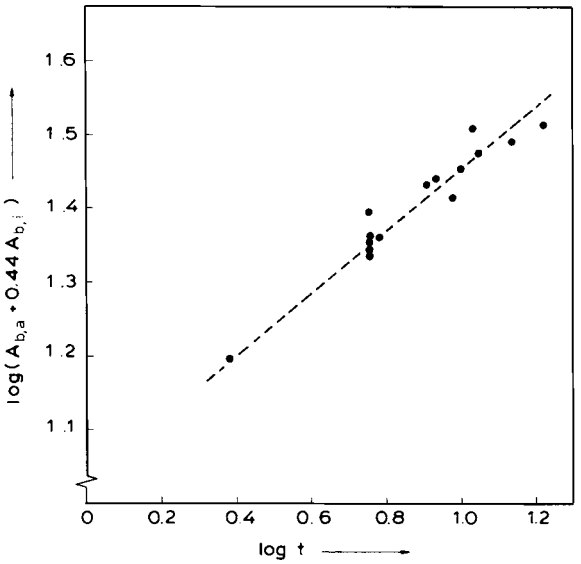

Fig. 10. Influence of yarn count on the total benzene absorbance at about 875 cm^{-1}.

In a separate experiment a variety of yarns with different counts were measured. The quantity log $(A_{b,a} + 0.44A_{b,i})$ was plotted vs. log t. In Figure 10 the experimental results show the straight line to be expected. For n the value of 0.42 was found, which confirms reasonably well the theoretical prediction that $n = 0.5$, as presented in Appendix A. This means that the absorbance is proportional to the yarn diameter and not to the area of the cross section. Based on these findings, in our computer program all isotropic areas are normalized by taking

$$A_n = \frac{A_{\text{iso}}}{A_{b,a} + 0.44A_{b,i}} \tag{6}$$

where A_n indicates the normalized isotropic area.

The benzene band at 793 cm^{-1}, often used for normalizing purposes, is less suitable as it definitely depends on crystallinity. Its isotropic area decreases with increasing crystallinity. Also its dichroic behavior points to a mainly amorphous character.

Dichroism

From the dichroism of an infrared band, the orientation of that part of the molecule which takes part in the vibration mode involved, can be obtained. The dichroic ratios are calculated as

$$D = A_{\parallel}/A_{\perp} \tag{7}$$

with $A_{\parallel}$ and $A_{\perp}$ indicating the integrated area of the absorbance peak for the parallel and perpendicular spectrum, respectively. From this D value

the Herman's orientation function can be calculated according to Samuels[1]:

$$f = \frac{3 < \cos^2 \theta > -1}{2} = \frac{(D-1)(D_0+2)}{(D+2)(D_0-1)} \tag{8}$$

where D_0 represents the dichroic ratio for the perfectly oriented molecular species concerned. The D_0 value depends on the angle between the transition moment and the molecular axis. This relation can be written[1] as

$$D_0 = 2 \cot^2 \alpha \tag{9}$$

where α is the transition moment angle. When $\alpha = 54.7°$, corresponding to $D_0 = 1$, dichroism cannot be used to determine the orientation factor. Positive orientation factors correspond with D values greater than 1 when $\alpha < 54.7°$ (π-bands) and with D values between 1 and 0 for $\alpha > 54.7°$ (σ-bands). As an example of the latter type of dichroism, in Figure 11 the orientation function f of the benzene out of plane vibration of the associated molecules at 873.5 cm^{-1} is given as a function of winding speed and elongation. For the calculations the value 0 is used for D_0. It can be seen that at low winding speeds the value of f approaches zero and the course of the orientation factor suggests that at speeds lower than 2000 m/min a negative orientation of the associated benzene molecules is achieved. Physically this means that the orientation of the majority of the associated benzene parts of the molecules is more perpendicular than parallel to the fiber axis at low takeup velocities. As these associated molecules can be regarded as the nuclei for thermal crystallization, this result can be considered to be in accordance with the finding of Liska.[27] He found that after crystallization

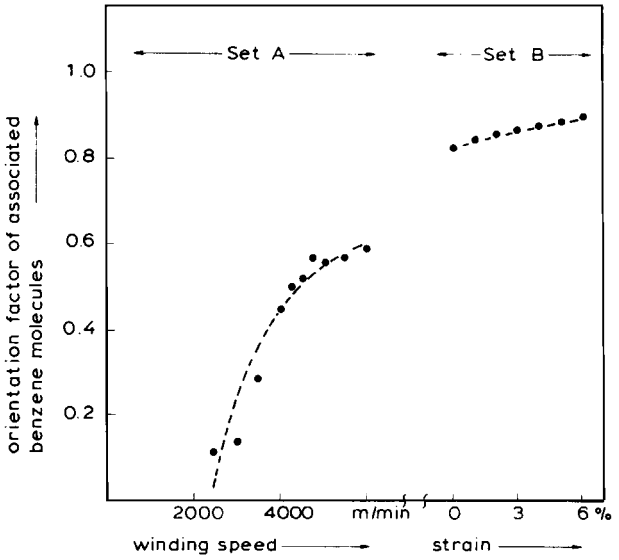

Fig. 11. Orientation function of the associated benzene molecules as a function of winding speed and elongation.

of initially amorphous yarns, wound at low speeds, resulted in yarns with a negative birefringence.

Numerical Summary of All Pearson VII Lines Involved

In Table III the numerical data of all 23 bands, used for describing a very wide range of PET fibers, is given. Not all parameters could be fixed as some need a certain range of variation between narrow limits. For some of these cases there is a physical reason for this as illustrated by the variable peak position of the "972" cm^{-1} trans bands discussed before. For some other cases it simply turned out that definite fixation was not possible without getting numerical trouble. For bands without physical interest to us, this situation has not been further investigated. In Figure 12 examples are given of the fitting results of a parallel and perpendicular infrared transmission spectrum of a commercial tyre yarn. It will be seen that the experimental points are described very well by the model used. The excellent fit and the small trouble near 1030 cm^{-1} in the parallel spectrum are representative of the many, i.e. some hundreds, yarn spectra that have so far been fitted with this method. The computing time on a Harris H500 machine for fitting a parallel and perpendicular spectrum simultaneously amounts to about 10 min. In Figure 13 plots are presented, where the deconvolution of the total absorbance, corresponding to the transmission given in Figure 12, is shown.

TABLE III

Peak position (cm^{-1})	Halfwidth (cm^{-1})	Shape factor	Dichroic character	Band assignment
1105.0	25.0	1.46	π	
1043.4	19.2	1.9	σ	Gauche
1023.5	25.0	1.3	π	
1018.0	7.1	1.8	π	
989.0	8.0	1.0	π	Fold
966.0–972.0	11.7	1.7	π	Trans
960.0–976.0	30.0	1.7	π	Trans
940.0	30.0	1.98	π	
924.0	25.0	1.98	π	
907.0	35.0	1.98	π	
898.5	17.5	1.9	π	Gauche
877.0	21.0	1.9	σ	Benzene
873.5	9.5	1.2	σ	Benzene
857.0	16.5	1.98	σ	
846.0–850.0	13.0	1.7	π	Trans
840.5	33.0	1.6	π	
816.0	15.0	1.98	π	
806.0	7.0	1.98	π	
798.0	35.0	1.98	σ	
792.3	8.0	1.6	π	Benzene
770.0–782.0	20.0–45.0	1.0	π	
745.0–765.0	22.0	1.0	π	
728.0–735.0	5.0–20.0	1.7	σ	

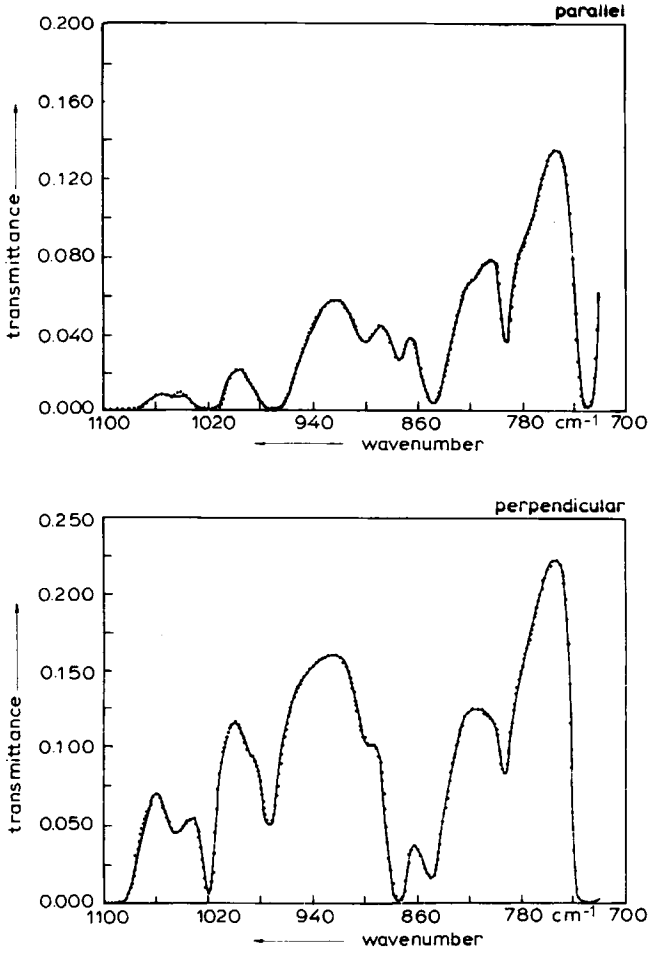

Fig. 12. Fitting results of a parallel and perpendicular spectrum of a PET tyre yarn: (· · · · ·) experimental values; (—) fitted model.

USE AND INTERPRETATION OF VARIOUS BANDS

Only a small part of the bands presented in Table III can be physically described. The assignments given are based on a combination of literature data and our own experience. The dichroic characters, as found experimentally from the fitting calculations, are also presented in the table. The most important bands will now be discussed, especially in relation to the initial aim of this infrared work. This aim was to gain more insight into folding at the boundaries of the crystals and into the chain length distribution of the tie molecules.

The first aspect turned out to be rather simple because the fold-band at 989 cm^{-1}, indicated in the literature,[4] could well be described by the model and its parameters were sufficiently well determined, as illustrated in Figure 15(b). The behavior of this band is in complete agreement with the assignment of Statton, Koenig, and Hannon. The tie-chain length distribution is a much more complicated subject. In the following the band assignments for trans and gauche as proposed by Ward et al.[11-13] will be used.

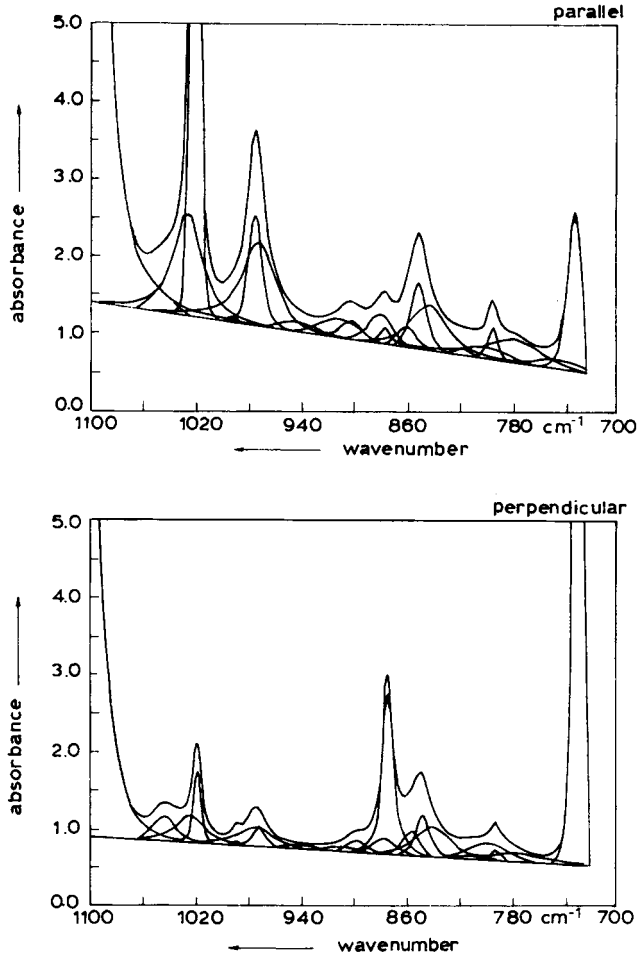

Fig. 13. Deconvolution of the total absorbance into its components.

Application of these assignments to our experimental results leads to a physically consistent model. First it should be realized that in the amorphous regions gauche as well as trans conformers are present. From Figure 14, it will be evident that a bend in a molecule requires some gauche parts, whereas straight molecules can only be composed of trans conformers. So the study of the trans and gauche bands provides more detailed information about the amorphous regions. Especially the decrease of the gauche bands at elongation provides information about the tie molecules. If, for example, at high elongation still an appreciable amount of the gauche conformer is present, it follows that the tie-chain length distribution is broad. Of course, not all gauche structures are long loops in tie molecules. A certain amount of nontie molecules as oligomers and matrix molecules will always be present. However, for a relative scaling the amount of gauche conformers is a useful indicator for the tie-chain length distribution. Information about the stress on the amorphous molecules can be obtained from the shift of the 972 cm^{-1} broad band. This information, however, is of a qualitative nature because the shift for a molecule depends on its chain length between successive crystals and consequently a distribution of shifts arises. The peak

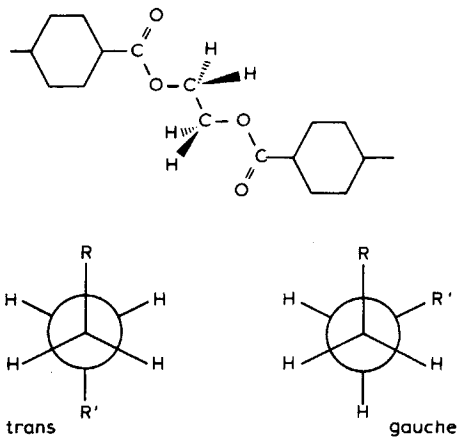

Fig. 14. Trans and gauche conformers of PET.

is therefore only a poor indicator of the average shift and probably the peaks at 940 and 924 cm^{-1} are needed to describe the skewing of the 972-amorphous band. A trial to use a really skew line shape for the description of the 972 cm^{-1} trans amorphous band was not successful because of numerical problems. Combining the shift of the crystalline 972 cm^{-1} component with the elongation of the unit cell as found with X-ray diffraction (see Fig. 8), one would expect an originally taut tie molecule at a macroscopic strain of 6% somewhere near 930 cm^{-1}. As the isotropic areas of the broad 940 and 924 cm^{-1} bands are not very accurate, this cannot clearly be supported experimentally.

Besides the fact that the original aim could be reached to a large extent, also another unexpected feature was found. The careful decomposition of the perpendicular benzene ring vibration near 875 cm^{-1} appeared to allow the detection of association of molecules at a level far below that detectable by x-ray diffraction. So even nuclei manifest themselves by the narrow band at 873.5 cm^{-1}.

The crystalline band near 848.5 cm^{-1} turned out to be very reliable for measuring crystallinities. It is well linearly related to crystallinities measured by the combination of X-ray diffraction and density.[2] Finally we report the remarkable sensitivity of the 1018 cm^{-1} band to elongation. Its π-dichroism and its isotropic area increase sharply, i.e., by a factor of 3–5, at an elongation of 6%. Maybe this is a benzene ring vibration, taking place in the direction of the molecule, which requires a fully planar configuration between benzene ring and aliphatic part of the molecule.

APPLICATIONS

Although some examples have already been presented in the foregoing part, yet various examples remain to be shown. Set A, the as-spun yarns wound at various speeds, is especially interesting with respect to orientation and crystallization processes during winding. As the samples of series B all originate from only one tyre yarn, they are of limited interest from a structural point of view. Therefore, examples taken from the results obtained

with the three yarns of set C were preferred. These examples show that the effect of strain on the infrared spectra is essential to demonstrate the structural differences of the three yarns as brought about by the different winding speeds.

Undrawn Yarns, Wound at Various Speeds

In Figure 15(a) the normalized isotropic area of the crystalline component at 848.5 cm^{-1} has been given as a function of the winding speed. The course is completely analogous to that of the crystallinity obtained from X-ray diffraction and densities as published before.[3] In Figure 15(b) the isotropic area of the fold-band is presented. It will be seen that the number of folds

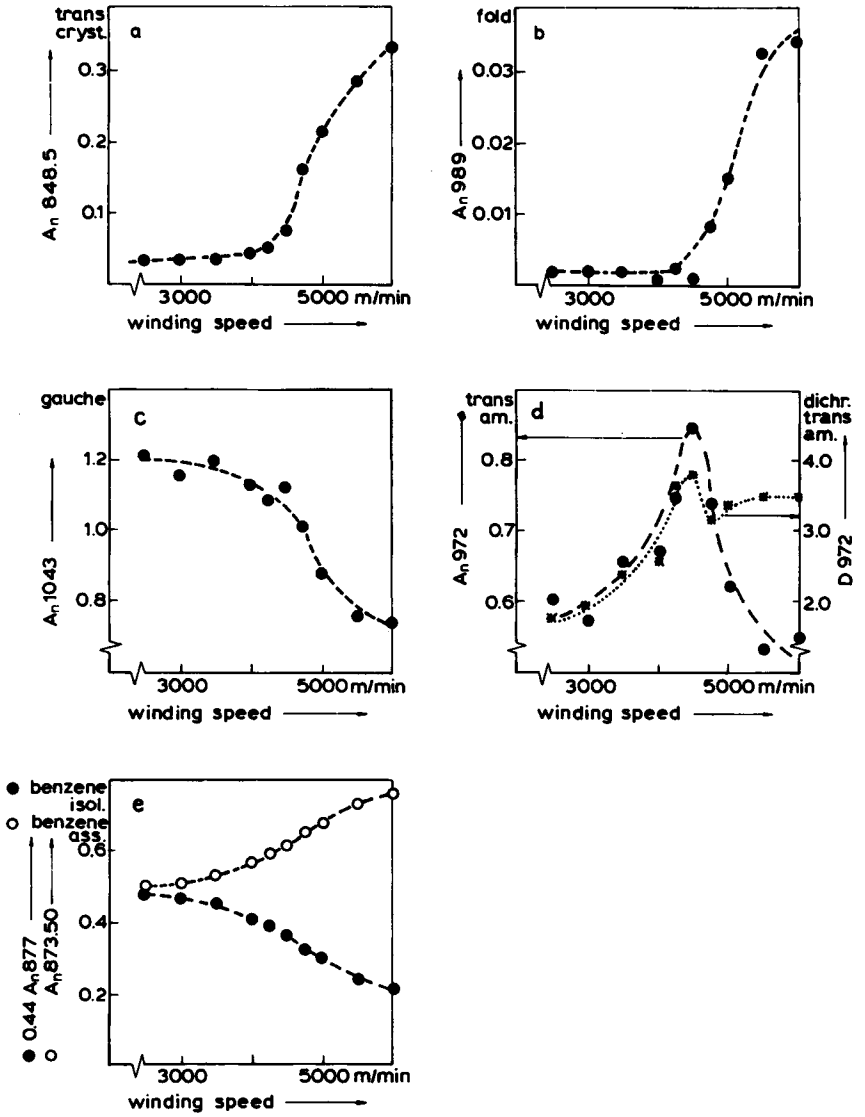

Fig. 15. Effect of winding speed on various infrared quantities of *undrawn* yarns.

increases with crystallinity. In Figure 15(c) the gauche content shows a decrease with increasing winding speed. First, up to about 4000 mpm, there is a gradual but slow decrease caused by increasing orientation in the amorphous yarns. Above that speed the decrease is steeper due to crystallization.

Figure 15(d) shows the course of the relative amount of the amorphous trans conformer and its dichroism. Up to the point where crystallization starts, the amount of the amorphous trans molecules increases due to increasing orientation and therefore increasing uncoiling of the amorphous molecules. This uncoiling and straightening of the molecules will cause gauche to trans transitions and therefore an increase of the amorphous trans content. As during the fast crystallization process, which takes place during winding at high speeds, the all-trans crystals will preferably incorporate the best oriented amorphous trans segments, the amount of amorphous trans will decrease sharply with the onset of crystallization. At still higher speeds, orientation and hence uncoiling and straightening will predominate. Dichroism is in full agreement with this point of view. First the orientation increases with winding speeds but crystallization causes a depletion of the best oriented amorphous molecules. These molecules are incorporated into crystals with a dichroic ratio of 5.7. Finally the amounts of "associated" and "isolated" benzene parts are given in Figure 15(e). As described before, the weighing factor of the broad component with respect to the narrow one, could be determined as 0.44. So in Figure 15(e) real percentages are presented. At low speeds there are about equal amounts of bundlelike and isolated species. At higher winding speeds the formation of bundles is favored and the narrow infrared band increases at the expense of the broader one. Orientation factors of the associated molecules have already been presented in Figure 11, showing an increase of orientation with winding speed. From the dichroism of the isolated molecules, it follows that their position becomes more and more perpendicular to the fiber axis at higher winding speeds. Probably it is these parts of the molecules, with a more or less perpendicular direction, which cannot be bundled by orientation and therefore remain present as "isolated" benzene parts.

Samples of One Tyre Yarn Wound at Various Elongations

In the foregoing this set served the study of the effect of straining on the infrared spectra and the interpretation of the spectral changes observed. The shift of the 972 cm^{-1} band, due to an increase of stress on the amorphous molecules at increased strain was presented in Figure 7. Also the effect of strain on orientation has already been illustrated in Figure 11. There are more spectral changes on straining worthwhile to be mentioned. Especially the decrease of the amount of gauche conformer on straining is a spectacular illustration of the uncoiling of molecules in the amorphous regions. However, the strength of this technique can best be illustrated by examples derived from set C. In that case three different yarns are involved. Not only examples in the unstrained state are presented, but also the response on straining is shown to be essential for the characterization of the differences in molecular structure of these three yarns.

Drawn Yarns Spun at Various Speeds and Wound at Various Elongations

For this set of yarns it should first be emphasized that the viscosity is higher than that of the as-spun yarns of series A. At a higher viscosity, crystallization takes place at a lower take-up velocity. For the viscosity concerned, the onset of crystallization is already at about 1700 mpm. So the yarns have been drawn from as-spun materials with a crystallinity varying from zero (at 500 mpm), via low (at 2000 mpm) to high (at 4000 mpm). This difference in crystallinity does not vanish completely during drawing. Of course, drawing enhances crystallinity substantially for all three situations. Nevertheless crystallinity and fold content, also after drawing, still increase with winding speed, as can be seen from the Figures 16(a) and (b). In Figures 16(c), (d), and (e), the course of the gauche content during elongation is illustrated for three different yarns. The first one drawn from the as-spun material, wound at 500 mpm, contains a relatively low amount of gauche conformers. The yarns spun at higher winding speeds reveal an increasing amount of gauche content. This indicates that the higher the winding speed of the undrawn starting material, the more molecular bends and coils are incorporated into the structure. Even more striking is the finding that in the low speed yarn the molecules can be uncoiled effectively, whereas this is impossible for the yarns originally wound at high speeds.

This means that the high-speed spun yarn contains very big loose loops which cannot be straightened upon straining to the elongations applied. Figures 16(f)–(h) show the behavior of the 972 cm^{-1} peak position of the amorphous trans parts of the molecules. No gradual change of the slope of the lines is found, but it is clear that the material wound at higher speeds contains stressed molecules already in the unstrained situation. So the picture emerges of a physical structure which depends largely on the winding speed of the as-spun starting material. High winding speeds cause an increase of folding, of the number of big loose loops and of the stress on the taut tie molecules. The first two phenomena possibly cause the lower strength and the latter the higher initial modulus, which is specific of this kind of yarns, as reported by Brody[16] already.

APPENDIX A: THEORETICAL CONSIDERATIONS ON THE TRANSMITTANCE THROUGH TWO LAYERS OF YARNS WITH CIRCULAR CROSS SECTIONS

In our experiments the yarns are very carefully wound on metal frames to form a smooth layer of parallel aligned filaments, on both sides of the frame. No embedding liquid is used because reproducible wetting of the wound yarns turns out to be very difficult and the excellent sensitivity of modern ratio recording spectrometers makes the use of embedding liquids superfluous. Moreover, a possible plasticizing effect of a liquid is thus avoided. Consequently, the influence of the circular shape of the cross section of the yarn on the light path of the infrared rays had to be studied extensively. The results are illustrated in Figure 17, where the light paths of various rays have been depicted. An incident beam of parallel infrared rays falls on the filaments of the first layer, passes through the polymer, and merges as a fully scattered diffuse radiation. Taking into account the uniform radiation density throughout the cross section of the incident infrared beam, the relative occurrence of the various light paths through a filament can be calculated. Weighing the light paths with the corresponding probabilities, it was found that the average length of the paths of the infrared rays through the

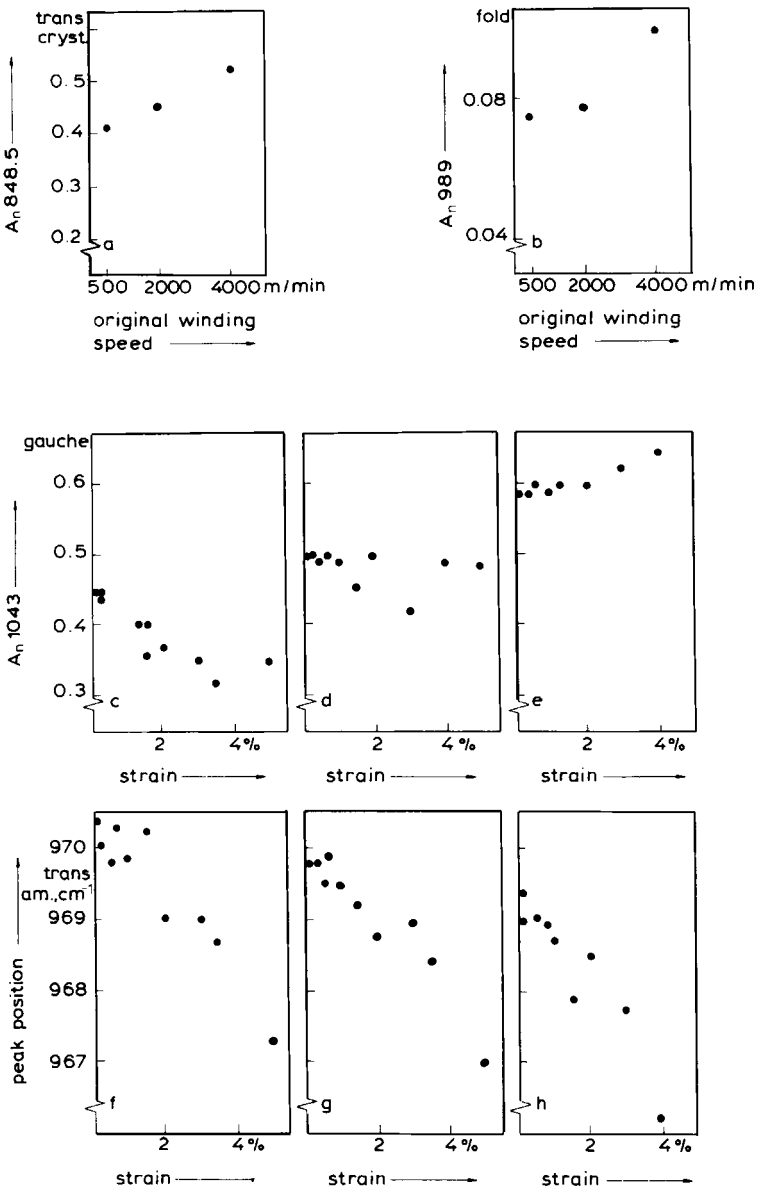

Fig. 16. Various infrared parameters of *drawn* yarns as functions of winding speed and strain.

cross section of the filament is about 96% of the diameter. This diffuse radiation hits the second layer. As indicated in Figure 17, the direction of the rays emerging from this second layer depends mainly on the point where they enter a filament. The line, connecting that point with the center of the circular cross section, is the main direction of the emerging rays. Calculations showed that the maximum deviation from this direction was not more than about 5° for a refractive index of 1.7. The average light path through the filaments of the second layer is calculated to be about 97% of the diameter. As the detection system is only reached by infrared rays emerging nearly parallel to the direction of the original incident infrared beam, it follows that only a small part of the emerging radiation is detected. These detected rays cover at least 93% of the maximum possible light path of twice the diameter through

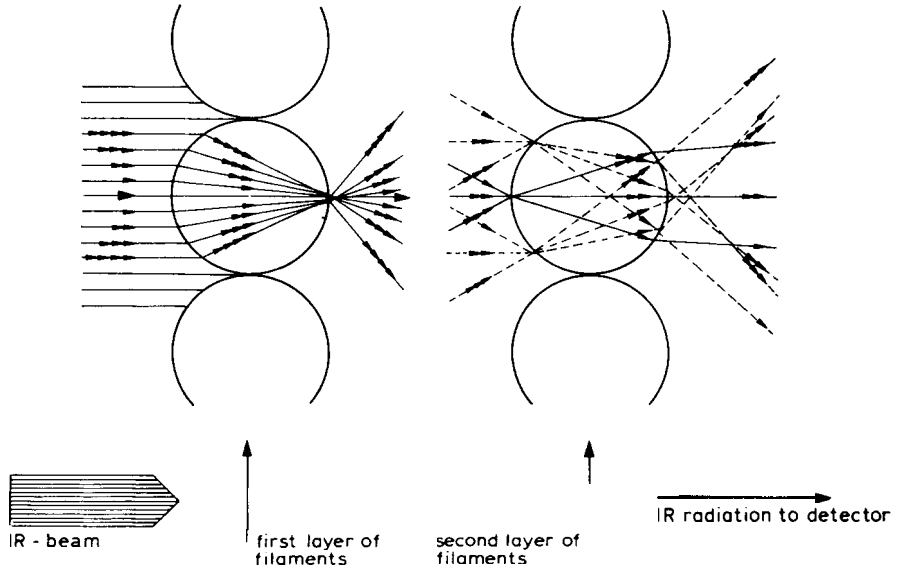

Fig. 17. Light path of infrared rays through the two yarn layers.

the filaments. This conclusion is in agreement with the observation mentioned in the subsection Normalized Isotropic Areas of the chapter Development of a fitting model that the isotropic absorbance by the total amount of benzene rings is nearly proportional to the square root of the filament count. If the whole cross section would contribute, a direct proportionality with the filament count and not with its square root would be expected.

The incident infrared beam is in the actual situation not exactly parallel but has a divergence of about 6°. Calculations showed that this does not substantially affect the aforementioned conclusions. For reflection considerations, a distinction has to be made between the two polarization directions. The rays polarized parallel to the fiber axis show an average reflection of about 10% (refractive index 1.7), whereas the rays whose direction of polarization is perpendicular to the fiber axis (refractive index 1.5) are reflected by only 2 or 3%. This difference in reflection does not affect the values of the dichroisms as these quantities are calculated from peak areas whereas reflections only influence the base lines. Multiple internal reflections can be neglected because this contribution has been proved to be extremely small.

The main conclusions of the foregoing are that, because of divergence, only a small part of the emerging infrared rays reach the detector of the spectrometer and that the detected rays cover about 93% of the maximum light path of twice the diameter through the filaments.

APPENDIX B: MATHEMATICAL FORMULATION OF THE INFRARED SPECTRA OF YARNS

Following the infrared through both layers of filaments, the following formula can be derived:

$$T = C \cdot T_{exp}^{1/2} \tag{10}$$

where T = transmission due to the absorption processes in the polymer, C = proportionality constant, slightly dependent on the wavenumber, and T_{exp} = the experimentally observed value of the transmission including all scattering and reflection effects due to the round shape of the yarn cross sections. In the constant C the effects of divergence and reflection at the four air–polymer boundaries are incorporated. As the reflections depend on the refractive index and the latter quantity may depend on the wavenumber, C has been formulated as wavenumber-dependent. For C equation

$$\log C = p + q\sigma \tag{11}$$

has been chosen, representing a linear base line to the absorbance, as this formulation turned out to be most satisfactory in fitting the spectra. The parameters p and q have to be obtained by the total fitting procedure as both may vary from sample to sample. Anomalous dispersion cannot be taken into account in this way; however, in the spectral region studied no problems of this kind have been encountered. This is probably due to the fact that in our spectra no extremely heavy bands are involved. If some radiation leaks through gaps between the filaments, only a relation between T and T_{exp} can be derived containing parameters which cannot be readily obtained experimentally, thus making a straightforward calculation of T from T_{exp} impossible. Therefore, leakage light should be avoided. This can easily be tested in the spectrometer by comparing the transmission at a zero transmittance band with that obtained with the incident beam blocked. If no leakage light is present, both readings are the same.

The transmission T can be described as 10^{-A}, where A is the absorbance. Said absorbance, composed of many molecular processes of infrared absorptions, can be described as $A = \sum_i P_i$ with P_i standing for Pearson lines describing the various molecular transitions with their own characteristic parameters. That these processes can only be added as absorbances is due to Beer's law. Combining the expressions for T and C, it follows

$$T_{exp} = 10^{-2[p+q\sigma+\sum_i P_i(\sigma)]} \tag{12}$$

The formula is equivalent to (10), apart from the factor 2 in the exponent. This factor is not relevant as it drops out by normalization and can therefore be omitted.

In actual calculations the transmission spectrum is fitted and not the related absorbance spectrum. This is because in transmission the scatter of the measuring points is nearly independent of the transmission level, resulting in a statistical equivalence of all measuring points as stressed already before by Pitha and Jones.[28]

The authors are extremely grateful to J. G. Westra who did the first infrared work on PET in our company, screened the possibilities for yarns and introduced us into this field. We also gratefully acknowledge the large contributions of J. L. Salve and M. Mannee who developed the complicated computer programs and of L. J. Lucas for his very skilled work on winding the filaments. We also like to mention the confidence and interest of A. Bezemer and J. M. Woestenenk who enabled us to do this work.

References

1. R. J. Samuels, *Structural Polymer Properties,* Wiley-Interscience, New York, 1974.
2. R. Huisman and H. M. Heuvel, *J. Appl. Polym. Sci.*, **22**, 943 (1978).
3. H. M. Heuvel and R. Huisman, *J. Appl. Polym. Sci.*, **22**, 2229 (1978).
4. W. O. Statton, J. L. Koenig, and M. Hannon, *J. Appl. Phys.*, **41**, 4290 (1970).
5. V. I. Vettegren, and I. I. Novak, *J. Polym. Sci., Polym. Phys. Eds.*, **11**, 2135 (1973).
6. S. N. Zhurkov, V. I. Vettegren, I. I. Novak, and K. N. Kashincheva, *Dokl. Akad. Nauk USSR*, **176**, 623 (1967).
7. K. K. R. Mocherla and W. O. Statton, *J. Appl. Polym. Sci, Appl. Polym. Symp.*, **31**, 183 (1977).
8. K. J. Friedland, V. A. Marikhin, L. P. Myasnikova, and V. I. Vettegren, *J. Polym. Sci., Polym. Symp.*, **58**, 158 (1977).
9. V. M. Voroboyev, I. V. Razumovskaya, and V. I. Vettegren, *Polymer*, **19**, 1267 (1978).
10. R. P. Wool, *Polym. Eng. Sci.*, **20**, 805 (1980).
11. I. M. Ward, *Chem. Ind.*, **1956**, 905.
12. I. M. Ward, *Chem. Ind.*, **1957**, 1102.
13. D. Grime and I. M. Ward, *Trans. Faraday Soc.*, **54**, 959 (1958).
14. W. W. Daniels and R. E. Kitson, *J. Polym. Sci.*, **33**, 161 (1958).
15. A. Garton, D. J. Carlsson and D. M. Wiles, *Text. Res. J.*, **51**, 28 (1981).
16. H. Brody, *J. Macromol. Sci. Phys.*, **B22**(1), 19 (1983).

17. H. Brody, *J. Mocromol. Sci. Phys.*, **B22**(3), 407 (1983).
18. H. M. Heuvel, R. Huisman, and K. C. J. B. Lind, *J. Polym. Sci., Polym. Phys. Ed*, **14**, 921 (1976).
19. M. M. Hall, *J. Appl. Cryst.*, **10**, 66 (1977).
20. A. J. Melveger, *J. Polym. Sci., A-2*, **10**, 317 (1972).
21. J. G. Westra and H. Wuestman, unpublished result.
22. L. D'esposito and J. L. Koenig, *J. Polym. Sci, Polym. Phys. Ed.*, **14**, 1731 (1976).
23. I. J. Hutchinson, I. M. Ward, H. A. Willis, and V. Zichy, *Polymer*, **21**, 55 (1980).
24. S. A. Baranova, S. A. Gribanov, B. N. Klyushnik, P. M. Pakhomov, V. E. Geller, and M. V. Shablygin, *Polym. Sci. USSR*, **25**, 333 (1983).
25. K. K. R. Mocherla, thesis, University of Utah, 1976.
26. A. Wasiak and A. Ziabicki, *Appl. Polym. Symp.*, **27**, 111 (1975).
27. E. Liska, Kolloid-Z., **251**, 1028 (1973).
28. J. Pitha and R. N. Jones, *Can. J. Chem.*, **44**, 3031 (1966).

Received September 10, 1984
Accepted November 30, 1984